A Robust and Efficient Power Series Method for Tracing PV Curves

Xiaoming Chen, David Bromberg, Xin Li, Lawrence Pileggi, and Gabriela Hug
Electrical and Computer Engineering Department, Carnegie Mellon University
5000 Forbes Avenue, Pittsburgh, PA 15213, USA
{xchen3, dbromber, xinli, pileggi, ghug}@ece.cmu.edu

***Abstract*—Estimating the voltage collapse point of a power grid is an important problem in power flow analysis. In this paper, we propose a novel power series method (PSM) for tracing the power-voltage (PV) curve and estimating the collapse point. By expanding the power flow equation into power series, a new point on the PV curve can be accurately extrapolated based on a previously solved point. Both forward stepping and backward stepping are proposed so that the proposed PSM can trace both the upper and lower halves of the PV curve. The collapse point is estimated as the intersection of the two half curves. Compared with the conventional continuation method, our PSM is numerically more robust. Compared with the conventional embedding method, our PSM offers superior accuracy and low computational cost.**

Keywords*—*Power Flow, Power Series Method (PSM), Collapse Point, Power-Voltage (PV) Curve

I. Introduction

Power flow analysis is one of the most important problems in power system operation as it not only provides information about the flows in the system but also assesses if the operating condition is secure and stable. Ensuring voltage stability is a serious concern to the electric utility industry [1]. Hence, for a given power system, it is essential to know the power-voltage (PV) curve and the maximum loadability, so that a secure and stable operating point can be determined and to know how close to voltage collapse the system is.

The Newton-Raphson (NR) method is widely used to solve power flow problems due to its quadratic convergence speed [2]. However, it is well-known that the Jacobian matrix of the power flow equation is singular at the maximum loading point [3]. As a result, the NR method fails to converge when the load is at or near the maximum loading condition, which is actually a voltage collapse point.

To overcome this singularity problem, continuation power flow (CPF) [4] was developed. The CPF method takes a homotopic approach by embedding an additional variable into the power flow equation to remove the singularity of the Jacobian matrix, which allows tracing the PV curve around the collapse point. Although many heuristics [5]–[7] have been studied in recent years to improve the CPF method, it has been pointed out that the extended Jacobian matrix posed by the CPF method may be poorly conditioned under specific loading conditions [8]. Once such a singularity issue occurs, the CPF method cannot accurately trace the PV curve and fails to find the collapse point.

In recent years, several novel power flow methods have been proposed. E.g., to overcome the convergence problem of conventional power flow solvers, a non-iterative holomorphic embedding load flow method (HELM) [9] was recently developed. The convergence of HELM is guaranteed by applying analytical continuation on the complex plane of holomorphic functions, if the power flow equation has a solution. As a result, HELM does not suffer from the singularity problem at the collapse point. Modeling generator buses in HELM was studied in [10]. The authors of [11] propose to remove the singularity of the Jacobian matrix by changing a PQ bus to a new AQ bus. However, like the CPF method, it does not theoretically guarantee that the singularity issue can be completely avoided at any point on the PV curve in general. Finally, a machine learning algorithm to calculate the collapse point is proposed in [12]. Such a learning-based approach needs a lot of data for training and collecting the required training data can be computationally expensive. In addition, it can only obtain the collapse point but cannot trace the entire PV curve.

This paper proposes a novel power series method (PSM) to robustly and efficiently trace the PV curve and calculate the collapse point. The PSM approximates the bus voltages as polynomial functions based on power series, similar (but not identical) to the conventional holomorphic embedding method [9]. As a result, the PV curve and the collapse point can be accurately estimated without suffering from any singularity issue.

In addition, to make the PSM computationally efficient, a number of implementation details are carefully studied. First, the Padé approximant is adopted to accurately predict the bus voltages based on the proposed power series model. It is expected to offer substantially improved accuracy over a simple polynomial model, as is demonstrated in the literature [13]. Second, a new stepping scheme is developed to quickly trace the PV curve where the step size is optimally controlled by the convergence domain of the power series. By exploiting the symmetric property of the PV curve near the collapse point [14], the proposed stepping scheme can estimate the full PV curve both accurately and efficiently. As will be demonstrated by the experimental results in Section IV, our proposed PSM offers superior performance (i.e., improved convergence, enhanced accuracy, and reduced runtime) over other conventional techniques.

The rest of this paper is organized as follows. In Section II we present the mathematical formulation of the PSM and then discuss the PSM-based curve tracing method in Section III. The efficacy of the PSM is demonstrated by a number of standard test cases in Section IV. Finally, we conclude in Section V.

II. Power Series Method

In this section, we present the foundation of the proposed PSM. We will explain the mathematical formulation for the power flow equation, develop the efficient numerical solver,

and finally describe the method to accurately estimate the voltages at all buses.

A. Overview

The power flow equation can be expressed as a set of nonlinear equations $\mathbf{f}(\mathbf{x})=\mathbf{y}$ [15]. Let's assume that we have a known solution $\mathbf{x}^{(old)}$ when the right-hand-side (RHS) is $\mathbf{y}^{(old)}$. Now, we change the RHS from the old value $\mathbf{y}^{(old)}$ to a new value $\mathbf{y}^{(new)}$, and, hence, the solution $\mathbf{x}$ should also be changed. The purpose of the proposed PSM is to find the updated solution $\mathbf{x}^{(new)}$ by solving the new power flow equation $\mathbf{f}(\mathbf{x}^{(new)}) = \mathbf{y}^{(new)}$ based on the known operating point $\mathbf{f}(\mathbf{x}^{(old)})=\mathbf{y}^{(old)}$.

To calculate the new solution $\mathbf{x}^{(new)}$, we follow the multilinear theory proposed in [16]. We first express the RHS $\mathbf{y}$ as the linear combination of $\mathbf{y}^{(old)}$ and $\mathbf{y}^{(new)}-\mathbf{y}^{(old)}$:

$$\mathbf{y} = \mathbf{y}^{(old)} + u\left(\mathbf{y}^{(new)} - \mathbf{y}^{(old)}\right), \tag{1}$$

where u is a real number. In (1), we conceptually apply an incremental update $u\left(\mathbf{y}^{(new)}-\mathbf{y}^{(old)}\right)$ to the old RHS $\mathbf{y}^{(old)}$ and then obtain the RHS $\mathbf{y}$. When $u=1$, $\mathbf{y}$ equals $\mathbf{y}^{(new)}$ and it represents the RHS of the power flow equation that we aim to solve. Once the RHS is changed from $\mathbf{y}^{(old)}$ to $\mathbf{y}$, the solution $\mathbf{x}$ is expressed as a power series with respect to u:

$$\mathbf{x} = \mathbf{x}^{(old)} + \sum_{k=1}^{\infty} u^k \mathbf{x}[k]. \tag{2}$$

Substituting (1) and (2) into the power flow equation yields:

$$\mathbf{f}\left(\mathbf{x}^{(old)} + \sum_{k=1}^{\infty} u^k \mathbf{x}[k]\right) = \mathbf{y}^{(old)} + u\left(\mathbf{y}^{(new)} - \mathbf{y}^{(old)}\right). \tag{3}$$

The physical meaning of (3) is obvious: if $u=0$, the solution is trivially the known operating point $\mathbf{x}^{(old)}$; if $u=1$, the solution satisfies the new power flow equation $\mathbf{f}(\mathbf{x}^{(new)})=\mathbf{y}^{(new)}$.

If each component of the vector $\mathbf{f}$ is a polynomial function of $\mathbf{x}$, then the left and right sides of (3) are both polynomials of u. As a result, the kth-order coefficients of the solution $\mathbf{x}[k]$ ($k = 1, 2, \cdots$) can be computed by equating the coefficients of the polynomials on both sides of (3). In what follows, we will show the detailed mathematical equations for PQ, PV and slack buses respectively. We will first start from first-order equations and then extend these equations to high-order cases. Our approach adopts the rectangular coordinate expression of the power flow equation, because the left side of (3) is not simply polynomial if the bus voltages are represented in their polar forms (i.e., by magnitudes and angles).

B. First-Order Power Series Expansion

1) PQ Bus: A PQ bus is described by two balance equations, namely balances of the active and reactive power:

$$e_i \sum_{j=1}^{N} (G_{ij}e_j - B_{ij}f_j) + f_i \sum_{j=1}^{N} (G_{ij}f_j + B_{ij}e_j) = P_i, \tag{4}$$

$$f_i \sum_{j=1}^{N} (G_{ij}e_j - B_{ij}f_j) - e_i \sum_{j=1}^{N} (G_{ij}f_j + B_{ij}e_j) = Q_i, \tag{5}$$

where

- e_i and f_i are the real and imaginary parts of the complex voltage of bus i;
- G_{ij} and B_{ij} are the series conductance and susceptance of the line between buses i and j;
- P_i and Q_i are the active and reactive power injections at bus i.

Since (4) and (5) are in the same form, we will take (4) as an example to show the detailed mathematical representations for the PSM. Once we understand the power series expansion for (4), the formulation for (5) can be derived in a similar way.

The voltage vectors $\mathbf{e}$ and $\mathbf{f}$ are both expressed as power series, i.e.,

$$e_i = e_i^{(old)} + \sum_{k=1}^{\infty} u^k e_i[k], f_i = f_i^{(old)} + \sum_{k=1}^{\infty} u^k f_i[k]. \tag{6}$$

Equating the first-order coefficients of (4) yields:

$$\begin{aligned} &e_i^{(old)} \sum_{j=1}^{N} (G_{ij}e_j[1] - B_{ij}f_j[1]) + \\ &e_i[1] \sum_{j=1}^{N} \left(G_{ij}e_j^{(old)} - B_{ij}f_j^{(old)}\right) + \\ &f_i^{(old)} \sum_{j=1}^{N} (G_{ij}f_j[1] + B_{ij}e_j[1]) + \\ &f_i[1] \sum_{j=1}^{N} \left(G_{ij}f_j^{(old)} + B_{ij}e_j^{(old)}\right) = {P_i}^{(new)} - P_i^{(old)}. \end{aligned} \tag{7}$$

2) PV Bus: A PV bus is described by a balance equation of the active power and another equation specifying the voltage magnitude, i.e.,

$$e_i \sum_{j=1}^{N} (G_{ij}e_j - B_{ij}f_j) + f_i \sum_{j=1}^{N} (G_{ij}f_j + B_{ij}e_j) = P_i, \tag{8}$$

$$e_i^2 + f_i^2 = V_i^2, \tag{9}$$

where V_i is the given voltage magnitude of PV bus i. As (8) is identical to (4), we will describe the detailed mathematical representations for (9) only. Similarly, equating the first-order coefficients of (9) yields:

$$2e_i^{(old)}e_i[1] + 2f_i^{(old)}f_i[1] = \left(V_i^{(new)}\right)^2 - \left(V_i^{(old)}\right)^2. \tag{10}$$

3) Slack Bus: The slack bus does not require power series expansion since its voltage is given and constant:

$$e_{sl} = 1, f_{sl} = 0. \tag{11}$$

where sl is the index of the slack bus.

4) Numerical Solver: Gathering all the first-order equations (i.e., (7), (10) and (11), and the power series expansion for (5) and (8)) together yields a linear system:

$$\mathbf{J}\mathbf{x}[1] = \mathbf{y}^{(new)} - \mathbf{y}^{(old)}, \tag{12}$$

where $\mathbf{J}$ is the Jacobian matrix of the power system at the known operating point $\mathbf{f}(\mathbf{x}^{(old)}) = \mathbf{y}^{(old)}$. The first-order coefficients of the solution $\mathbf{x}[1]$ can be solved from (12) by a linear sparse solver [17].

C. High-Order Power Series Expansion

High-order power series expansion is handled in a way similar to the first-order case.

1) PQ Bus: Equating the nth-order ($n > 1$) coefficients of (4) yields:

$$\begin{aligned} &e_i^{(old)} \sum_{j=1}^{N} (G_{ij}e_j[n] - B_{ij}f_j[n]) + \\ &e_i[n] \sum_{j=1}^{N} \left(G_{ij}e_j^{(old)} - B_{ij}f_j^{(old)}\right) + \\ &f_i^{(old)} \sum_{j=1}^{N} (G_{ij}f_j[n] + B_{ij}e_j[n]) + \\ &f_i[n] \sum_{j=1}^{N} \left(G_{ij}f_j^{(old)} + B_{ij}e_j^{(old)}\right) = \Delta P_i(n), \end{aligned} \tag{13}$$

where

$$\Delta P_i(n) = -\sum_{k=1}^{n-1} \begin{bmatrix} e_i[k] \sum_{j=1}^{N} (G_{ij}e_j[n-k] - B_{ij}f_j[n-k]) \\ +f_i[k] \sum_{j=1}^{N} (G_{ij}f_j[n-k] + B_{ij}e_j[n-k]) \end{bmatrix},$$

which only depends on the lower-order coefficients of the solution.

2) PV Bus: Equating the nth-order coefficients of (9) yields:

$$2e_i^{(old)}e_i[n] + 2f_i^{(old)}f_i[n] = \Delta V_i^2(n), \tag{14}$$

where

$$\Delta V_i^2(n) = -\sum_{k=1}^{n-1} (e_i[k]e_i[n-k] + f_i[k]f_i[n-k]),$$

which also only depends on the lower-order coefficients of the solution.

3) Numerical Solver: The left-hand-side (LHS) of (7) and (13) are identical except that the coefficient order is changed from 1 to n. The same conclusion also holds for (10) and (14). Consequently, combining all the nth-order equations yields a similar linear system:

$$\mathbf{J}\mathbf{x}[n] = \Delta\mathbf{y}(n), \tag{15}$$

where the RHS $\Delta\mathbf{y}(n)$ only depends on the lower-order coefficients of the solution. The nth-order coefficients of the solution $\mathbf{x}[n]$ can be solved from (15) by a linear solver [17], when the coefficients of the solution from the first-order to $(n-1)$th-order are all known. To determine the coefficients at different orders, (15) is repeatedly solved by incrementally increasing n. It is important to note that (12) and (15) share the same Jacobian matrix $\mathbf{J}$. Hence, even though (15) must be solved repeatedly, we only need to factorize the Jacobian matrix $\mathbf{J}$ once when solving (12) and the matrix factors can then be reused to solve (15).

D. Voltage Estimation

When the coefficients up to a given order are all obtained, the voltages of all buses are estimated by evaluating the power series at $u = 1$. In our implementation, we do not directly sum the power series at $u = 1$. Instead, we adopt the Padé approximant to improve the estimation accuracy. The Padé approximant uses a rational fraction to approximate a bus voltage x as a function of u, i.e.,

$$x[0]+x[1]u+\cdots+x[L+M]u^{L+M} \approx \frac{a[0]+a[1]u+\cdots+a[L]u^L}{1+b[1]u+\cdots+b[M]u^M}, \tag{16}$$

where $x[\cdot]$ denotes the coefficients of a bus voltage. Typically, the diagonal ($L = M$) or near-diagonal ($|L-M| = 1$) Padé approximant yields the maximal analytic continuation and thus, gives the most accurate estimation [13]. The detailed algorithm to calculate the Padé approximant can be found in the literature, e.g., [13]. Once the Padé approximant for a bus voltage is known, the voltage value can be estimated by setting u=1 on the RHS of (16).

E. Summary

The proposed PSM solves the power flow equation based on a known operating point by power series expansion. The proposed PSM includes five major steps:

1) Construct the Jacobian matrix $\mathbf{J}$ at the known operating point and form (12);
2) Perform LU factorization for the Jacobian matrix $\mathbf{J}$;
3) Solve the first-order coefficients of the solution $\mathbf{x}[1]$ by (12);
4) Repeatedly solve the high-order coefficients of the solution $\mathbf{x}[n]$ by (15). Incrementally increase n until a given order is reached;
5) Estimate the bus voltages by the Padé approximant (16).

The proposed PSM has a convergence domain which depends on the expansion point (i.e., the known operating point) and the highest order of the power series. That is also to say, it is not possible to accurately solve the new power flow equation with an arbitrary RHS $\mathbf{y}^{(new)}$. We will discuss the details of this issue in Section III-B.

III. Tracing the PV Curve

In this section, we present an efficient algorithm to trace the PV curve and estimate the collapse point using the proposed PSM. We will develop the robust curve tracing algorithm, explain the step size control strategy, describe the method to estimate the collapse point, and finally summarize the major steps for our proposed algorithm.

A. Forward Stepping

Before tracing the PV curve, we need to solve the power flow equation at a starting point, which is referred to as the base case. The load of the base case should be sufficiently small so that a physical solution exists on the upper half of the PV curve and it can be reliably found by a conventional power flow solver (e.g., the NR method).

Given the base case, the PV curve is traced by changing the power components on the RHS of the power flow equation. Without loss of generality, the RHS of the power flow equation is expressed as the sum of the base case and the change in the load, i.e.,

$$\mathbf{f}(\mathbf{x}) = \mathbf{y}^{(m)} = \mathbf{y}_{base} + \lambda^{(m)}\mathbf{y}_{ch}, \tag{17}$$

where the superscript $^{(m)}$ denotes the iteration number, $\mathbf{y}_{base}$ represents the base case, $\mathbf{y}_{ch}$ is the change in real and reactive load power demand and real power generation, and $\lambda^{(m)}$ stands for the loading factor to specify the amount of load change.

For two consecutive iterations, (17) can be transformed into a form that is similar to (1):

$$\mathbf{f}(\mathbf{x}) = \mathbf{y} = \mathbf{y}_{base} + \lambda^{(m)}\mathbf{y}_{ch} + u\left(\lambda^{(m+1)} - \lambda^{(m)}\right)\mathbf{y}_{ch}. \tag{18}$$

When u=0, $\mathbf{y}$=$\mathbf{y}_{base}$+$\lambda^{(m)}\mathbf{y}_{ch}$=$\mathbf{y}^{(m)}$ corresponds to $\mathbf{y}^{(old)}$; when $u = 1$, $\mathbf{y} = \mathbf{y}_{base} + \lambda^{(m+1)}\mathbf{y}_{ch} = \mathbf{y}^{(m+1)}$ corresponds to $\mathbf{y}^{(new)}$. Hence, the proposed PSM can be used to solve the power flow equation at the $(m+1)$-th iteration by expanding

the solution using the power series at the mth iteration. Starting from the base case for which the physical solution sits on the upper half of the PV curve, the complete upper half curve can be traced by incrementally increasing the loading factor over iterations.

B. Step Size Estimation

The step size $(\lambda^{(m+1)}-\lambda^{(m)})$ of the loading factor affects the accuracy of the solution at the $(m+1)$-th iteration. In order to appropriately choose the optimal step size, we first study the truncation error of our proposed power series and then further map the truncation error to the residual of the power flow equation. The step size is computed such that the residual is less than or equal to a given threshold, and thus, the accuracy is guaranteed. Note that numerical errors are ignored in our analysis.

1) Truncation Error of the Power Series: The power series expansion of bus voltages $\mathbf{x}$ is equivalent to the Taylor expansion of the inverse function of $\mathbf{f}(\mathbf{x})=\mathbf{y}$, which is denoted as $\mathbf{x}=\mathbf{g}(\mathbf{y})$. Consequently, the truncation error of the power series is equivalent to the Lagrange remainder of the nth-order Taylor expansion [18]:

$$R_i\Big(\lambda^{(m+1)},n\Big)=\sum_{\alpha_1+\cdots+\alpha_N=n+1}\left[\frac{\prod_{j=1}^{N}\frac{\partial^{\alpha_j}g_i(\widetilde{\mathbf{y}})}{\partial y_j^{\alpha_j}}}{\prod_{j=1}^{N}\alpha_j!}\prod_{j=1}^{N}(\Delta y_j)^{\alpha_j}\right], \quad (19)$$

where Δy_j is the jth component of $(\lambda^{(m+1)}-\lambda^{(m)})\mathbf{y}_{ch}$, and $\widetilde{\mathbf{y}}$ is a point in the open ball $\mathbf{B}\big(\mathbf{y}^{(m)};|\mathbf{y}^{(m+1)}-\mathbf{y}^{(m)}|\big)$. The truncation error in (19) is represented as a function of the loading factor $\lambda^{(m+1)}$ and the order of the expansion. As the loading factor $\lambda^{(m+1)}$ and, hence, the step size $\lambda^{(m+1)}-\lambda^{(m)}$ increase, the truncation error is expected to increase. For this reason, we must choose a sufficiently small step size to guarantee high approximation accuracy at each iteration step. Given (19), it remains difficult to directly estimate the remainder, because we do not know the exact value of $\widetilde{\mathbf{y}}$ in practice. However, the following equation can be derived from (19):

$$\frac{R_i\left(\lambda^{(m+1,a)},n\right)}{R_i\left(\lambda^{(m+1,b)},n\right)}\approx\left(\frac{\lambda^{(m+1,a)}-\lambda^{(m)}}{\lambda^{(m+1,b)}-\lambda^{(m)}}\right)^{n+1}, \quad (20)$$

where $\lambda^{(m+1,a)}$ and $\lambda^{(m+1,b)}$ are two different values for the loading factor. In what follows, we will further use (20) to derive the relation between the residual of the power flow equation and the step size $\lambda^{(m+1)}-\lambda^{(m)}$ in order to appropriately estimate the optimal step size.

2) Residual of the Power Flow Equation: To simplify our notation, we take (4) as an example to analyze the residual of the power flow equation. Let δe_i and δf_i be the truncation error of e_i and f_i, respectively. If the error is sufficiently small and the second-order terms (i.e., $\delta e_i\cdot\delta e_j$, $\delta e_i\cdot\delta f_j$, and $\delta f_i\cdot\delta f_j$) are ignored, the residual of (4) is expressed as:

$$\|f_i(\mathbf{x})-P_i\|_2=\left\|\begin{matrix}e_i\sum_{j=1}^{N}(G_{ij}\delta e_j-B_{ij}\delta f_j)+\delta e_i\sum_{j=1}^{N}(G_{ij}e_j-B_{ij}f_j)\\+f_i\sum_{j=1}^{N}(G_{ij}\delta f_j+B_{ij}\delta e_j)+\delta f_j\sum_{j=1}^{N}(G_{ij}f_j+B_{ij}e_j)\end{matrix}\right\|_2. \quad (21)$$

Equation (21) implies that the residual of the power flow equation $\|\mathbf{f}(\mathbf{x})-\mathbf{y}\|_2$ is approximatively a linear function of the truncation error δe_i and δf_i. Let $Res(\delta\mathbf{x})$ be the residual of the power flow equation associated with the truncation error $\delta\mathbf{x}$. We have:

$$Res(\beta\cdot\delta\mathbf{x})\approx\beta\cdot Res(\delta\mathbf{x}), \quad (22)$$

where β is a constant. Combining (20) and (22) yields the following equality:

$$\frac{Res\left(\mathbf{R}\left(\lambda^{(m+1,a)},n\right)\right)}{Res\left(\mathbf{R}\left(\lambda^{(m+1,b)},n\right)\right)}\approx\left(\frac{\lambda^{(m+1,a)}-\lambda^{(m)}}{\lambda^{(m+1,b)}-\lambda^{(m)}}\right)^{n+1}. \quad (23)$$

3) Step Size Prediction: The step size is estimated based on (23). As a heuristic, we first tentatively solve the coefficients of the power series expansion at an empirically selected loading factor $\lambda^{(m+1,pre)}=\lambda^{(m)}+0.2\left(\lambda^{(m)}-\lambda^{(m-1)}\right)$. The highest order coefficient $\mathbf{x}[n]$ is set as the truncation error $\mathbf{R}\big(\lambda^{(m+1,pre)},n\big)$. Then, the residual $Res\big(\mathbf{R}\big(\lambda^{(m+1,pre)},n\big)\big)$ is calculated using (21). Finally, to ensure that the residual at $\lambda^{(m+1)}$ equals to the given threshold eps, $\lambda^{(m+1)}$ is calculated using (23):

$$\lambda^{(m+1)}=\lambda^{(m)}+\left(\lambda^{(m+1,pre)}-\lambda^{(m)}\right)\left(\frac{eps}{Res\big(\mathbf{R}\big(\lambda^{(m+1,pre)},n\big)\big)}\right)^{\frac{1}{n+1}}. \quad (24)$$

This method can generally guarantee a small residual as long as the expansion point is far away from the collapse point. Starting from the estimated loading factor $\lambda^{(m+1)}$ by (24), we continuously check the residual when a new point is solved. If the residual is larger than eps, we repeatedly reduce the step size by $\frac{1}{2}$ and resolve the the coefficients of the power series expansion. If the number of iterations exceeds a given limit but the residual remains larger than eps, it indicates that the current loading factor is overly large and the power system is very close to the collapse point. In this case, the forward stepping procedure ends and we will perform backward stepping in the next step.

C. Backward Stepping

To trace the lower half of the PV curve, a starting point on the lower half curve is required. It has been proven in the literature that the PV curve close to the collapse point is close to a quadratic function [14]. Therefore, in the neighbourhood of the collapse point, the upper half and lower half curves are nearly horizontally symmetric. For convenience, we label the last two points from forward stepping as A and B respectively, as shown in Fig. 1. Point B is the last point of forward stepping and, hence, it is close to the collapse point. Based on these two points A and B and the symmetric assumption, we can estimate a new point C on the lower half curve. As shown in Fig. 1, the voltages of the three points satisfy the following equation:

$$(e_A+e_C)\approx 2e_B,(f_A+f_C)\approx 2f_B, \quad (25)$$

where e and f stand for the real and imaginary parts of the voltage. Based on (25), we can obtain an "approximate" point on the lower half curve for each bus. Taking this predicted point as the initial guess, we further apply the NR method to solve the power flow equation, resulting in a solution that sits on the lower half of the actual PV curve.

Once we obtain the aforementioned starting point, we can trace the entire lower half of the PV curve by applying the same method that is used for forward stepping. Here, we gradually decrease the loading factor and solve the power flow equation by the proposed PSM until the loading factor is sufficiently small.

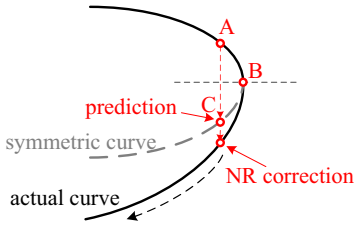

Fig. 1. Illustration of how to obtain a starting point on the lower half of the PV curve for backward stepping.

D. Collapse Point Estimation

Once we obtain both the upper and lower halves of the PV curve, we can estimate the collapse point of the power system by extrapolation. We first select a bus that has the largest slope between the last two points of the upper half curve [8]. We then form two straight lines based on the selected bus. One line passes through the last two points of the upper half curve of the selected bus and the other line passes through the last two points of the lower half curve of the selected bus. Finally the intersection point of the two lines is calculated as the collapse point.

IV. Experimental Results

For testing and comparison purposes, three different methods are implemented to trace PV curves: (i) the proposed PSM, (ii) the conventional embedding method that is similar to HELM [9], and (iii) the CPF method offered by MATPOWER [19]. Both the proposed PSM and the embedding method are implemented in C/C++ with the same step size to trace PV curves. As such, a fair comparison on both accuracy and runtime can be made for these methods. Eight test cases provided by MATPOWER are used. All experiments are performed on a desktop with an Intel i7 3.6GHz CPU and 16GB memory.

A. Comparison on Robustness

As mentioned in [8], the CPF method does not always work because the extended Jacobian matrix may be singular under specific loading conditions. To illustrate this limitation of CPF, we consider the test case with 3012 buses. In Fig. 2, we show the PV curves calculated by several different methods for the 741st bus. The CPF method fails in this example before the collapse point is reached. Fig. 3 shows the zoomed-in PV curves near the collapse point. It shows that the CPF method fails on the upper half of the PV curve when the loading factor is around 1.3597. In addition, due to the numerical

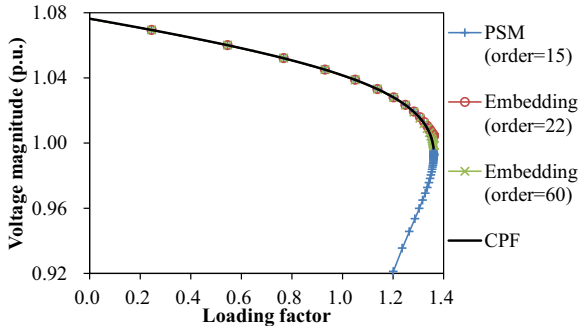

Fig. 2. The PV curves calculated by different methods are plotted for the 741st bus of the test case with 3012 buses.

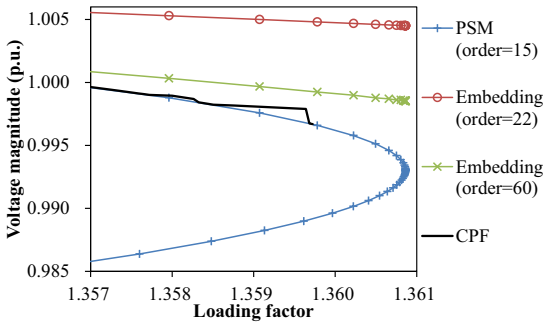

Fig. 3. The zoomed-in PV curves calculated by different methods are plotted for the 741th bus of the test case with 3012 buses.

issues caused by the singular Jacobian matrix, the PV curve obtained by CPF is not smooth around its failure point. Fig. 3 also shows that the conventional embedding method cannot accurately estimate the PV curve around the collapse point. Unlike the conventional methods, our proposed PSM traces the PV curve both accurately and robustly in this example. In what follows, we will further compare the accuracy and runtime between the different methods.

B. Comparison on Accuracy

We first compare the accuracy for the estimated PV curve between our PSM and the embedding method as shown in Table I. The accuracy is assessed by the maximum (MAX) error and the root-mean-square (RMS) error of the upper half of the PV curve. Here we only measure the error for the upper half curve, because the conventional embedding method was not particularly designed to detect the collapse point and trace the entire PV curve. In our experiment, the PV curve estimated by CPF is used as the golden solution for error calculation. The MAX error and the RMS error are defined as:

$$Error_{MAX} = \max_{1\le i\le P_t}\left\{\left|V_{PSM/Emb}(\lambda^{(i)}) - V_{CPF}(\lambda^{(i)})\right|\right\},$$
$$Error_{RMS} = \sqrt{\frac{1}{P_t}\sum_{i=1}^{P_t}\left(V_{PSM/Emb}(\lambda^{(i)}) - V_{CPF}(\lambda^{(i)})\right)^2}, \quad (26)$$

where $V_{PSM/Emb}(\lambda^{(i)})$ and $V_{CPF}(\lambda^{(i)})$ are the voltage magnitudes at the ith loading factor on the upper half curve estimated by the PSM/embedding method and the CPF method, respectively; P_t is the number of points on the upper half curve. Note that both the MAX error and RMS error of the embedding method are 3 to 6 orders of magnitude larger than those of our PSM. Even after the order is increased from 22 to 60 for the embedding method, the error does not significantly decrease.

In these examples, our proposed PSM achieves superior accuracy over the conventional embedding method due to the

TABLE I. Absolute Errors (p.u.) for Estimated PV Curves.

Case #	# of buses	Absolute error (PSM)		Absolute error (Embedding)			
		Order=15		Order=22		Order=60	
		MAX	RMS	MAX	RMS	MAX	RMS
1	39	4.46E-06	1.45E-06	3.18E-02	1.55E-02	1.17E-02	4.17E-03
2	57	1.30E-05	4.53E-06	2.66E-02	1.08E-02	7.45E-03	2.47E-03
3	118	1.74E-06	5.05E-07	3.20E-02	1.90E-02	1.25E-02	6.10E-03
4	300	3.86E-06	1.20E-06	3.83E-02	1.92E-02	1.50E-02	5.80E-03
5	2383	1.41E-06	3.65E-07	3.69E-02	1.65E-02	1.19E-02	4.70E-03
6	2746	3.11E-06	7.33E-07	6.42E-02	3.29E-02	2.59E-02	1.06E-02
7	3120	1.55E-07	3.84E-08	4.15E-02	2.47E-02	2.12E-02	1.07E-02

following reason: the PSM always solves a new point on the PV curve based on the power series expansion of the previous point. The proposed step size control method ensures the accuracy of the new point that is solved. On the contrary, the embedding method cannot easily take advantage of the solution at the previous point. For a given loading factor, the embedding method must rely on the expansion of a reference point at which the power flow equation becomes linear and, hence, trivially simple to solve (i.e., the no-load, no-generation case) [9]. Because the loading factor at the reference point can be significantly different from the given loading factor at the new point on the PV curve, extrapolating from the reference point to the new point often results in large errors.

We further verify the correctness and accuracy of our PSM based on the estimated collapse points. Table II compares the collapse points estimated by our PSM and the CPF method. Here the collapse points estimated by CPF are treated as the golden solution to evaluate the error for our PSM. Note that although CPF is treated as the golden solution, it may fail as shown in Fig. 3. As shown in Table II, the absolute error of our PSM is in the order of 10^{-8} to 10^{-4}. It, in turn, demonstrates that the PSM can robustly and accurately calculate the collapse points for these test cases.

C. Comparison on Runtime

Table III compares the runtime for estimating the upper half curve by our PSM and the embedding method, when both of them use the same step size. The embedding method with Order=22 has a similar computational cost as our PSM. When the order of the embedding method is increased to 60, it is about 7 to 8 times more expensive than our PSM. As shown in Table I, the maximum error and the RMS error of the embedding method are both much larger than those of our PSM. Based on these results, our PSM offers superior performance over the conventional embedding method.

V. Conclusion

In this paper, we propose a novel PSM to trace the PV curve and estimate the collapse point both efficiently and robustly. Towards this goal, bus voltages are approximated by power series such that an unknown point on the PV curve can be extrapolated based on a known point that is computed in the previous iteration step. A novel stepping scheme is developed to efficiently trace both the upper and lower halves of the PV curve where the step size is optimally controlled. Experimental results reveal that our proposed PSM offers enhanced robustness, superior accuracy and reduced runtime over the conventional CPF method and embedding method.

TABLE II. Collapse Points (a.u.) Estimated by PSM and CPF.

Case #	# of buses	PSM	CPF	Absolute error
1	39	1.135698	1.135697	1.50E-06
2	57	0.892091	0.891769	3.22E-04
3	118	2.187100	2.187100	1.16E-07
4	300	0.429341	0.429339	2.37E-06
5	2383	0.893713	0.893670	4.29E-05
6	2746	1.876904	1.876486	4.18E-04
7	3120	1.331414	1.331413	8.33E-08

TABLE III. Runtime (seconds) for estimating the upper half curve.

Case #	# of buses	PSM	Embedding	
		Order=15	Order=22	Order=60
1	39	0.0032	0.0037	0.0266
2	57	0.0046	0.0047	0.0334
3	118	0.0138	0.0145	0.1061
4	300	0.0266	0.0275	0.2072
5	2383	0.1601	0.1576	1.1299
6	2746	0.2347	0.2200	1.6176
7	3120	0.3137	0.3149	2.4128

VI. Acknowledgement

This research is supported in part by the CMU-SYSU Collaborative Innovation Research Center (CIRC) at Carnegie Mellon University.

References

[1] P. Kundur, N. J. Balu, and M. G. Lauby, *Power system stability and control*. New York: McGraw-hill, 1994, vol. 7.

[2] W. F. Tinney and C. Hart, "Power flow solution by Newton's method," *Power Apparatus and Systems, IEEE Transactions on*, vol. PAS-86, no. 11, pp. 1449–1460, Nov 1967.

[3] Y. Wang, L. da Silva, W. Xu, and Y. Zhang, "Analysis of ill-conditioned power-flow problems using voltage stability methodology," *Generation, Transmission and Distribution, IEE Proceedings-*, vol. 148, no. 5, pp. 384–390, Sep 2001.

[4] V. Ajjarapu and C. Christy, "The continuation power flow: a tool for steady state voltage stability analysis," *Power Systems, IEEE Transactions on*, vol. 7, no. 1, pp. 416–423, Feb 1992.

[5] Y. Ju, W. Wu, B. Zhang, and H. Sun, "Continuation power flow based on a novel local geometric parameterisation approach," *Generation, Transmission Distribution, IET*, vol. 8, no. 5, pp. 811–818, May 2014.

[6] A. Neto and D. Alves, "An improved parameterization technique for the continuation power flow," in *Transmission and Distribution Conference and Exposition, 2010 IEEE PES*, April 2010, pp. 1–6.

[7] X. Zhang and A. Flueck, "A geometric framework method for voltage stability analysis based on sensitivity analysis," in *North American Power Symposium (NAPS), 2012*, Sept 2012, pp. 1–6.

[8] J. Zhao and B. Zhang, "Reasons and countermeasures for computation failures of continuation power flow," in *Power Engineering Society General Meeting, 2006. IEEE*, 2006, pp. 1–6.

[9] A. Trias, "The holomorphic embedding load flow method," in *Power and Energy Society General Meeting, 2012 IEEE*, July 2012, pp. 1–8.

[10] M. Subramanian, Y. Feng, and D. Tylavsky, "PV bus modeling in a holomorphically embedded power-flow formulation," in *North American Power Symposium (NAPS), 2013*, Sept 2013, pp. 1–6.

[11] S. Ghiocel and J. Chow, "A power flow method using a new bus type for computing steady-state voltage stability margins," *Power Systems, IEEE Transactions on*, vol. 29, no. 2, pp. 958–965, March 2014.

[12] R. Zhang, Y. Xu, Z. Y. Dong, P. Zhang, and K. P. Wong, "Voltage stability margin prediction by ensemble based extreme learning machine," in *Power and Energy Society General Meeting (PES), 2013 IEEE*, July 2013, pp. 1–5.

[13] G. A. Baker and P. R. Graves-Morris, *Padé approximants*. Cambridge University Press, 1996, vol. 59.

[14] H.-D. Chiang, C.-S. Wang, and A. Flueck, "Look-ahead voltage and load margin contingency selection functions for large-scale power systems," *Power Systems, IEEE Transactions on*, vol. 12, no. 1, pp. 173–180, Feb 1997.

[15] F. Milano, *Power system modelling and scripting*. Springer Science & Business Media, 2010.

[16] M. Schetzen, "Multilinear theory of nonlinear networks," *Journal of the Franklin Institute*, vol. 320, no. 5, pp. 221 – 247, 1985.

[17] T. A. Davis, *Direct Methods for Sparse Linear Systems*. US: Society for Industrial and Applied Mathematics, 2006.

[18] M. Kline, *Calculus: an intuitive and physical approach*. Courier Corporation, 1998.

[19] R. Zimmerman, C. Murillo-Sanchez, and R. Thomas, "MATPOWER: Steady-state operations, planning, and analysis tools for power systems research and education," *Power Systems, IEEE Transactions on*, vol. 26, no. 1, pp. 12–19, Feb 2011.